CHAPTER 4 – DEFECT CHARACTERIZATION AND IMAGING

This chapter addresses the third task of the investigation regarding defect characterization. To accomplish this, changes in concrete velocities are correlated with the changes in concrete strength and 3-D strength images are provided. The correlation of field measured CSL velocities and laboratory measured concrete velocity values to concrete strength values is established, as described next. The laboratory values are acquired from ultrasonic pulse velocity (UPV) testing obtained from 5 concrete cylinders at 4, 7, 14, 21, and 28-day intervals.

4.1 ESTABLISHMENT OF EMPERICAL RELATIONSHIP BETWEEN CSL VELOCITY AND STRENGTH

In present drilled shaft construction practice, the unconfined compressive strength of concrete f'_c is in the range of 20,700- 34,500 kPa (3,000-5,000 psi) for normal density cast-in-place concrete. High strength concretes, with f'_c to about 82,800 kPa (12,000 psi), are used mostly for pre-stressed long-span bridges. The strength data is usually obtained through tests after 28 days after concrete placement.

The modulus of elasticity of concrete E_c (in units of psi) is defined as the slope of the initial straight portion of the stress-strain curve. For concretes with compressive strength to about 41,400 kPa (6,000 psi), the following empirical relationship from the ACI code is used (Nilson and Winter, 1986)[4]:

$$E_c = 33\,\rho_c^{1.5}\sqrt{f'_c} \qquad (4)$$

where f'_c is the strength in psi and ρ_c is density of hardened structural concrete (in lb/ft^3) in the range of 1.44-2.5 g/cm^3 (90-155 lb/ft^3). For normal sand-and-stone concretes, with ρ_c = 2.32 g/cm^3 (145 lb/ft^3), Equation (4) becomes:

$$E_c = 57{,}000\sqrt{f'_c} \qquad (5)$$

From the theory of elasticity, compressional wave velocity V_p in an homogeneous, isotropic and elastic media is given by:

$$V_p = \sqrt{(E_c / \rho_c)} \qquad (6)$$

In narrow bars with lateral dimensions comparable to the transmitted wavelength, V_p is extensional wave velocity and E_c becomes Young's modulus. Using Equations (5) and (6)

[4] This universal concrete modulus to strength relationship (4) is developed without a good (high) R^2 correlation value. This is obviously due to the vast variety of aggregates, cements, and additives used by the concrete industry. As described in Section 4.1.3, it is more desirable to develop a shaft-specific strength to modulus (or velocity) relationship.

$$f'_c \approx V_p^4 \ \rho_c^2 \qquad (7)$$

Therefore, a fourth power relationship is assumed between unconfined compressive strength of concrete and compressional wave velocity (and only a second power relationship with density). This fourth power velocity-strength relationship is the current industry standard. It is used to characterize defective concrete in drilled shafts typically of less than 28 days in age even though the above strength relationships is usually obtained through tests made 28 days after the concrete placement. It is also used herein in developing strength images in Chapter 5.

Obviously, using a universal relationship such as Equation (7) between velocity and strength is very desirable. However, as described in section 4.1.3, a shaft specific relationship between strength and velocity is preferred that is developed for concrete of less than 28 days in age.

4.1.1 Example Calculation

A defect zone with 20% drop in velocity ($V_{new} = 0.8\ V_{old}$) and using Equation (7) implies:

$$f_{new} \approx 0.8^4\ f_{old} = 0.4\ f_{old} \qquad (8)$$

Therefore, the strength in the defect zone is about 40% of old strength. Similarly, a concrete with a 10% drop in velocity implies the strength in the defect zone is 65% of old strength.

4.1.2 Current Industry Standards for Defect Definition

Using standard CSL or CSLT testing, "questionable" concrete condition is defined as a zone with a decrease (from median) in sonic velocity between 10% and 20% (or about 40%-65% of old strength); and, "poor" concrete condition is defined as a zone with greater than 20% decrease in sonic velocity (or about less than 40% of old strength). (Please refer to footnote 2 for example specification).

4.1.3 Empirical Relationship Between Core Strength and CSL Velocity

As mentioned above, developing a universal relationship that relates either the maturity parameters or velocity to strength parameters of concrete (such as Equation (7)) is, obviously very desirable. However, this is not typically achievable because of wide variations in three categories of parameters used in construction of a shaft (Yuan, Nazarian, and Medichetti, 2003), namely:

1. *Mix-Related Parameters* – Referring to the vast variety of aggregates, cements and additives that are used in the concrete industry;
2. *Environmental-Related Parameters* – Referring to varying subsurface conditions; specifically, changes in stiffness, moisture, and temperature;
3. *Construction-Related Parameters* – Referring to changes in shaft diameter and differing reinforcement designs.

In this study, Equation (7) is sought to be determined empirically for the same concrete mix used in the construction of the shaft. To that end, concrete cylinders from 20 different cylinders from the Sevenmile Gooseberry, Utah project were tested using the ultrasonic pulse velocity (UPV, ASTM-C597) method at 4, 7, 14, 21, and 28-day intervals, as described below.

4.1.3.1 Ultrasonic Pulse Velocity (UPV) Method

The ultrasonic pulse velocity (UPV) method determines the velocity of propagation of ultrasonic energy pulse through a concrete member by transmitting a short duration, high voltage resonant frequency signal by a pulser to a transducer coupled to the opposite concrete surface. When the pulse is received the timer is turned off and the elapsed travel time is measured. The pulse velocity is obtained by dividing the direct path length between the transducers by the travel time.

For a given concrete mixture, as the compressive strength increases with age, there is a proportionally smaller increase in the pulse velocity (Jones, 1954). At early ages (typically 2-7 days), the pulse velocity is very sensitive to the gain in strength.

UPV results are operator dependent and for longer travel paths the test results are not constant. The accuracy of measurements also depends on factors such as moisture content (Jones and Facaoaru, 1969) and density of steel reinforcement (Chung, 1978) in the concrete member.

The results of the laboratory UPV testing from the Sevenmile-Gooseberry Project are shown in Figures 21 and 22. In these figures, UPV testing was performed by two groups (Olson Engineering and CFLHD) which is referred to as Batch 1 and Batch 2. Compressive strength measurements were all obtained by CFLHD. Each group tested two (2) samples at each time interval for statistical considerations; however, UPV measurements were not performed at 4 day testing (only strength measurements). The fourth power velocity-strength curve is also shown. For such a limited range in strength values, a conclusive power relationship cannot be inferred.

4.1.3.2 Maturity Method

To obtain a more representative empirical relationship between velocity and strength, the maturity method (Saul, 1951) must be considered. The maturity method assumes: 1) concrete derives its strength from the hydration of cement; 2) this hydration of cement produces heat; 3) if one can monitor this heat, then an estimation of the extent of the hydration reaction can be made and—as a result—the strength of the concrete can be predicted. The temperature-time approach, described herein, approximates the heat production as the area under the temperature-time curve. From the measured maturity, the strength of a concrete mass is determined by reference to the previously determined relationship between maturity and strength.

Two different methods are described in ASTM C1074 for analyzing concrete maturity. The first is the temperature time factor method (TTF), which utilizes the Nurse-Saul equation (Saul, 1951) as:

$$M(t) = \sum (T_a - T_0)\Delta t \qquad (9)$$

Batch 1					
Sample	Age	Strength (kPa)	Strength (PSI)	Velocity (m/s)	Velocity (ft/s)
03-801-CC	7	31440	4560	4150	13615
03-802-CC	7	31030	4501	4160	13648
03-803-CC	14	34010	4933	4260	13976
03-804-CC	14	32900	4772	4220	13845
03-805-CC	21	35140	5097	4230	13878
03-806-CC	21	35330	5124	4160	13648
03-807-CC	28	37090	5379	4260	13976
03-808-CC	28	36320	5268	4260	13976

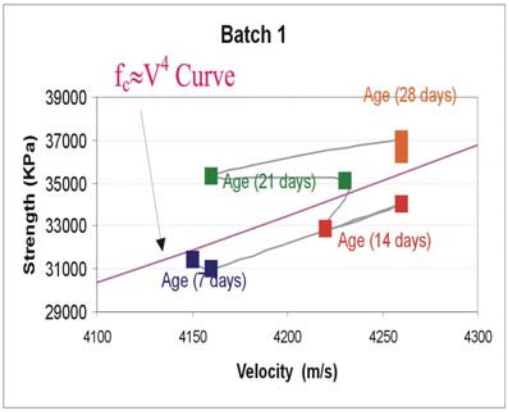

Figure 21. Chart. Velocity Versus. Strength Curve for Batch 1.

Batch 2					
Sample	Age	Strength (kPa)	Strength (PSI)	Velocity (m/s)	Velocity (ft/s)
03-811-CC	7	31370	4550	4140	13583
03-812-CC	7	30920	4485	4170	13681
03-813-CC	14	33090	4799	4210	13812
03-814-CC	14	32300	4685	4130	13550
03-815-CC	21	33680	4885	4270	14009
03-816-CC	21	35650	5171	4190	13747
03-817-CC	28	34270	4970	4280	14042
03-818-CC	28	35590	5162	4250	13944

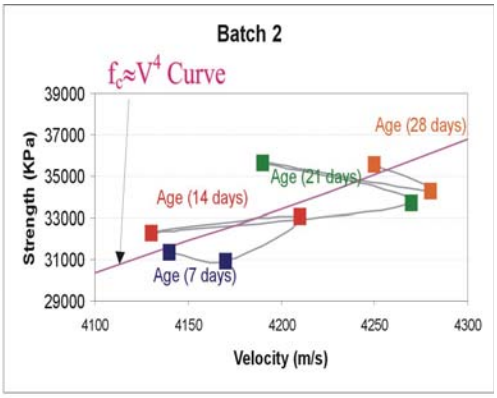

Figure 22. Chart. Velocity versus Strength Curve for Batch 2.

where M(t) is a "time-temperature factor" (TTF) at time t, T_0 is the lowest temperature at which a gain in strength is observed, T_a is the average temperature during time interval Δt between consecutive measurements. An examination of Equation 9 shows that it is an integration of the temperature-time curve utilizing the trapezoidal method. Basically, in this formulation, the maturity is the area under the temperature-time curve.

The second approach for analyzing maturity is the equivalent age (EQA) method, which is computed using the Nurse-Saul function as:

$$t_e = \sum \frac{(T_a - T_0)}{(T_r - T_0)} \Delta t \qquad (10)$$

where the equivalent age (t_e) is defined as the duration of the curing period at the reference temperature (T_r) resulting in the same maturity value as the curing period at any other temperature. Equation (10) can be written as:

$$t_e = \sum \alpha \Delta t \; ; \qquad (11)$$

where $\alpha = \frac{(T_a - T_0)}{(T_r - T_0)}$ is known as the age conversion factor as it converts Δt to the equivalent curing interval at the reference temperature. Alternatively, using the Arrhenius equation, Equation (10) becomes:

$$t_e = \sum e^{-Q\left(\frac{1}{T_a} - \frac{1}{T_r}\right)}.\Delta t \qquad (12)$$

where Q is the apparent activation energy divided by the universal gas constant. Like the TTF method, the equivalent age (EQA) method is an integration of time and temperature, except the temperature difference is embedded an exponential function.

Maturity measurement in the field primarily consists of monitoring the internal temperature of the concrete with respect to time by either a maturity meter or a temperature data-logger. Maturity meters are basically temperature-measuring devices that monitor temperature by attaching thermocouple wires inserted into the fresh concrete. ASTM C1074 summarizes the procedure for applying the maturity method as:

1) In the laboratory, a strength-maturity relationship is developed on the mixture to be used;
2) In the field, the temperature history of the concrete being tested is recorded from placement to the time the strength estimate is needed;
3) the maturity index is calculated; and
4) the strength at that maturity is estimated from the strength-maturity relationship.

For NDT testing programs of drilled shafts of less than 7 days in age, it is recommended to conduct a maturity and a UPV test in the laboratory prior to the strength test. A plot between the average compressive or flexural strengths and average maturity values (TTF value or equivalent age t_e) must be made and a best-fit curve obtained. The curve is used for estimating the strength of concrete based on maturity. Additionally, a plot between the average strengths and average velocity (or seismic modulus) and between average velocity and average maturity must be developed. The maturity method can then be used to compare CSL velocities, obtained at field cured temperature of less than 7 days in age, to the laboratory obtained UPV velocities as it is correlated to strength.

In addition to the above mentioned effect of temperature on velocity, several other correction factors needs to be considered, as is described next.

4.2 DIFFERENCES BETWEEN LABORATORY AND FIELD MEASUREMENTS

One important consideration is the disparity that exists between the laboratory measurement of ultrasonic pulse velocity (UPV) and CSL field derived velocity data. Specifically, it appears the UPV derived velocity from concrete cylinders to be significantly higher than field measurements of velocity using CSL method so that the entire shaft would be considered flawed. Some of the factors that are thought to be responsible for the differences between laboratory and field measurements include:

1. *Temperature Effects* – As described above, CSL field measured velocities in drilled shafts are obtained at field cured temperatures few days after the concrete placement where a non-linear temperature-dependent process affects velocity. Because the field derived CSL velocities are obtained at much higher temperatures than UPV velocities from laboratory (environmentally controlled) samples, higher UPV velocities are observed.
2. *Velocity Dispersion* - Dispersion refers to changes in sonic velocity as a function of frequency. Typically, CSL measurements are obtained around 40 kHz transducer frequencies. However UPV measurements are typically obtained at 58 kHz (as was done herein in Figures 21 and 22) resulting in higher measured UPV velocities. To correct this, it is recommended that UPV measurements be obtained using lower 40 kHz frequency transducers, which are available from NDT equipment manufacturer.
3. *Scale Factors* – For 1.2 m (4 ft) or larger diameter shafts, usually lower CSL velocities are observed in the perimeter path as compared to longer diagonal paths. One explanation for the difference of velocities with path length can be understood in terms of a self-similar (fractal) distribution of heterogeneities within the material. Therefore, a better averaging of velocities is obtained in long paths.
4. *Tube Effects* – For the perimeter paths, the effect of tube inside diameter (I.D.) and tube bending is more pronounced and must be considered as compared to the diagonal paths.
5. *Dissimilar Concrete Batches* – The field concrete is not always from the same batch proportions as the laboratory samples.

All these factors must be taken into consideration for determining the proper corrective factors that need to be applied to the laboratory data for proper calibration of the CSL/CSLT field derived velocity to concrete strength. However, the most dominant corrective factor is considered to be the temperature effects, which is described next.

4.3 TEMPERATURE MODELING

Concrete samples tested in the laboratory often show higher velocities than those inferred from CSL measurements made on shafts shortly after placement. As previously discussed in Section 4.2, one main reason for this discrepancy is the temperature difference of laboratory samples versus the much warmer concrete in a drilled shaft at the time of CSL testing. However, as described in Section 4.1.3.1, if the CSL data is compared of the same maturity as the cylinders, a better correlation is obtained.

In the next section, the results from computer-based modeling of the radial variations of temperature in drilled shafts are presented. Two-dimensional axisymmetric thermal models are computed for curing concrete shafts and samples, with the goal of understanding if these differences may arise from different thermal and curing states at the time of testing. To summarize, the laboratory samples are found to heat negligibly whereas the shafts remain warm for weeks. The dominant control on the thermal evolution of both small samples and large shafts is the primary curing period of a few days, during which most of the cement's latent heat is released. What little temperature increases can be sustained in the small samples is quickly

erased after this period, whereas the larger shafts require an additional several days to shed the bulk of their heat. Therefore, it is likely that CSL measurements made after several days to a week have elapsed since a shaft is placed will be more compatible with sample measurements. Otherwise, embedded thermocouples must be used to compare shaft velocities to laboratory sample velocities of the same maturity. In Section 4.4, a simple field experiment is described that can determine the minimum time after shaft placement when valid CSL measurements can be obtained, by repeating CSL measurements each day for a period of one week.

4.3.1 Method Used to Determine The Effect of Temperature on Velocity/Strength

The MATLAB 11 Partial Differential Equations Toolbox (Mathworks, 1998) was used to solve the parabolic (heat-flow) equation

$$(k/\rho C_p)\,\nabla^2 T = \partial T/\partial t + Q \qquad (13)$$

where T is the temperature, t is the time, k is the thermal conductivity ρ is the density, C_p is the specific heat at constant pressure, and Q is the volumetric heat production. The assumed physical parameters (adapted from Sims, 1999) are given in Table 2. The quantity κ (= $k/\rho C_p$) in Equation (13) is the thermal diffusivity and for the values selected here is $3\text{x}10^{-7}$ m^2 for concrete and $5\text{x}10^{-7}$ m^2 for earth. Therefore, heat will diffuse somewhat more readily into the ground surrounding a shaft, but not so much so that a distinct thermal boundary will remain between shaft and earth after some time.

Table 2. Material Properties.

Parameter	Concrete	Earth
Thermal conductivity k, W/m-K	1	2
Density ρ, kg/m3	3000	2000
Heat capacity C_p, J-kg/K	1000	2000

The volumetric heat production for concrete was estimated from Figure 3 in Gajda and VanGeem, 2002, for a mixture of 75% Type V cement + 25% Class F fly ash (with a total of 311 kg/m^3 (525 lb/yd^3) of cementitious materials). The adiabatic heating curve (Figure 23) was empirically fit with two linear segments. The slope of the lines is related to the heat production as

$$Q = \rho C_p\, dT/dt \qquad (14)$$

The assumed heat production due to concrete curing is then

$$Q = 675 \text{ W/m}^3,\ t < 2 \text{ days}$$
$$Q = 5.8 \text{ W/m}^3,\ t > 2 \text{ days} \qquad (15)$$

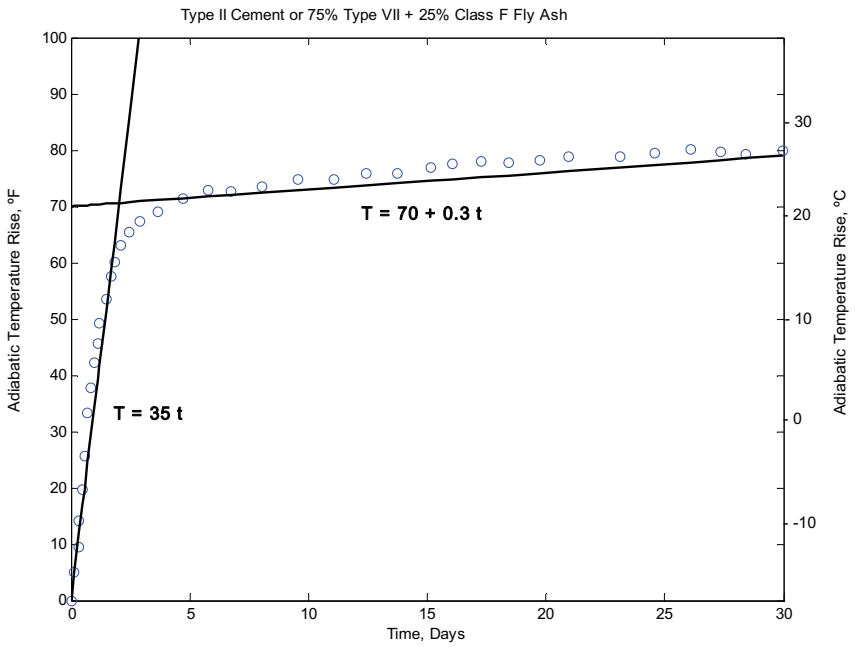

Figure 23. Plot. Adiabatic Temperature Increase vs. Time for Representative Concrete, with Approximate Linear Fits. Note Primary Curing Occurs In 2 Days.

Equation 13 was solved in two-dimensional axisymmetry. The assumed concrete shaft had a diameter of 1.5 m and a length of 10 m (4.9 x 32 ft). The assumed concrete sample had a diameter 15 cm and a length of 30 cm length (6 x 12 in). Both the sample and the shaft had zero heat flux specified across the central axis. For the sample, a film coefficient of 5 W/m^2K—appropriate to convective heat transfer to air (Welty et al., 1984)—was used at the outer boundaries. The air temperature was taken to be 0ºC (32ºF) for convenience. An alternative boundary condition that directly fixes the temperature of the outer wall of the sample at 0ºC (32ºF) is equivalent to an infinite film coefficient. No explicit boundary condition is needed at the shaft wall because it is assumed to be in contact with earth; the outer boundary of the modeled earth is, however, fixed to 0ºC (32ºF).

4.3.2 Temperature Modeling Results

Thermal models for small size concrete samples are shown in Figures 24 and 25 and models for larger size shafts are shown in Figures 26-28. The models for the samples illustrate the differences in boundary-condition assumptions: because the sample is small it has a short thermal response time of minutes to hours (time ~ $radius^2$/thermal diffusivity) and therefore the temperature distribution is strongly controlled by the interaction between internal heating and the boundary conditions. Regardless of which model is chosen, the maximum temperature increases are a few degrees Celsius and the sample cools rapidly after primary curing is completed in a few days.

The larger 1.5 m diameter shaft has a longer thermal response time (a few to several days) which, together with the insulating effect of surrounding earth, permits central peak temperatures in excess of 30ºC (86ºF) and mean temperatures of ~15ºC (59ºF) to develop. Note that the adiabatic temperature increase (i.e., for a perfectly insulated shaft) over the 2-day primary curing

period is ~40ºC (104ºF). Cooling in the shaft is commensurately slow, with temperatures exceeding the maxima observed in the sample (~5ºC (41ºF)) to persist for 3-4 weeks or greater. When curing retardants are added (to impede concrete curing process), the peak temperature is reduced, but the interaction between reduced peak temperature and longer cooling time approximately cancel with regard to the time over which elevated temperatures are observed. In other words, the cooling time to 5ºC (41ºF) is relatively unchanged.

In summary, concrete samples are expected to show only very small temperature increases with prompt cooling after primary curing is completed. For all practical purposes, the interior of concrete samples is therefore at ambient temperature when UPV measurements are performed. Concrete shafts show temperature increases of a few to several tens of degrees Celsius for the first week after concrete is placed, with mean temperatures in excess of the maximum observed in the sample to persist for a month or more. Therefore the shaft is always warm relative to the sample when UPV-CSL measurements are made in the field.

In solid rock—such as sandstone with similar properties as concrete—sound speed varies only slightly with temperature, of order 5%/100ºC (5%/212ºF) (Sheriff and Geldart, 1995). However, the sound speed in rocks saturated with heavy crude oil or tar varies as much as 20%/100ºC (20%/212ºF). For the maximum average temperature differences of a few-to-several tens of degrees Celsius modeled here between samples and shafts, velocity differences of only a few percent would be expected. In practice, mean shaft velocities derived from CSL can be >20% below sample measurements.

It is, therefore, possible that for concrete, there is a nonlinear temperature-dependent process affecting velocity, such as fluid interconnectivity or other strong dependence of elastic constants on curing state. During primary curing there is probably still extensive fluid interconnection. As many CSL measurements are made within a day after placement, concrete may be relatively solid but incompletely cured, and interconnected fluid pathways that persist at elevated temperatures of a few tens of degrees Celsius may reduce mean velocities. If CSL measurements are made after a few thermal response times following primary curing (i.e., ~7 days after placement), then any residual fluid is probably no longer interconnected and velocities are more comparable to those observed in samples. A simple field experiment was conducted and presented in Section 4.4 to examine these characteristics by repeat CSL measurements at intervals of a day and correlation with the temperature profiles.

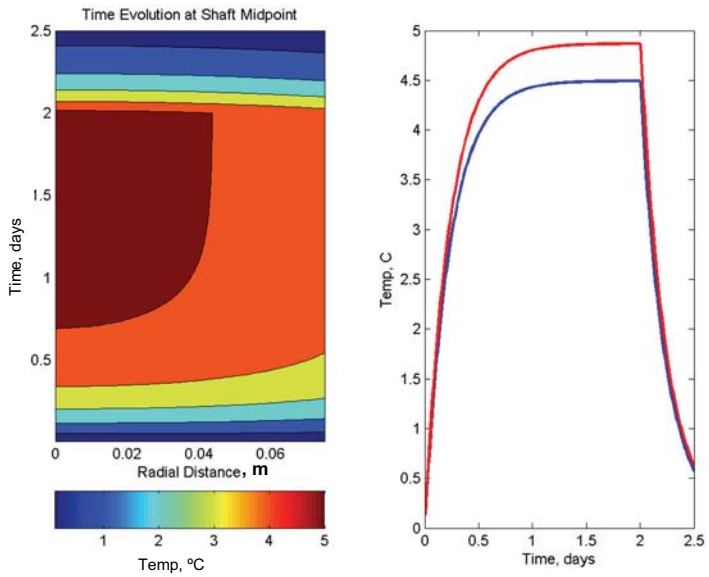

Figure 24. Chart. Thermal Evolution of 15 x 30 cm (6 x 12 in) Concrete Sample under Nominal Convective Cooling to Surrounding Air. Left: Radial Slices at Vertical Midpoint (i.e., at 15 cm (6 in) of 30 cm (12 in) length). Right: Upper Curve (Red) is Shaft Midpoint (Equivalent to Left Vertical Axis on Left-Hand Plot). Lower (Blue) Curve is Average Temperature in the Sample. Curves are Close because Boundary Layer to Convecting Air Effectively Retains Heat. Average Temperature Increase is < 5ºC.

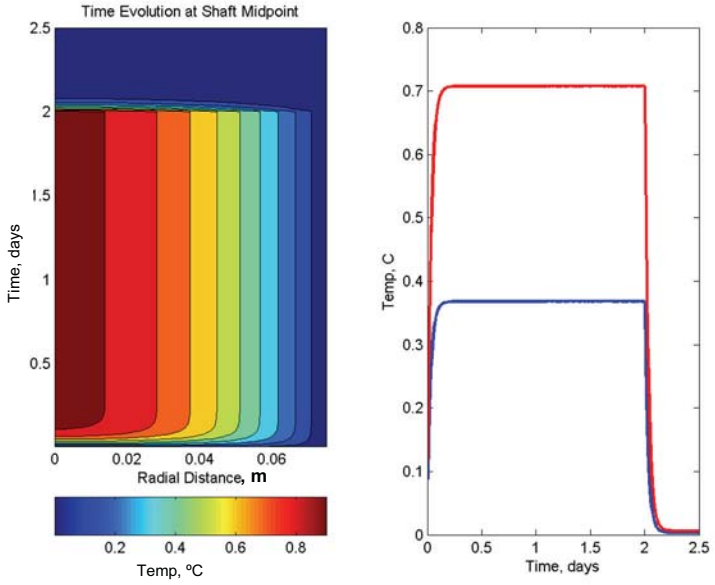

Figure 25. Chart. As Figure 24, but with Constant-Temperature Outer Boundary Condition, Appropriate to Maximally Efficient Convective Cooling to Surrounding Air. Note Strong Radial Temperature Gradients and Large Difference in Central Vs. Mean Temperatures because of Fixed-Temperature Boundary Condition. Maximum Temperature Increase is < 1ºC.

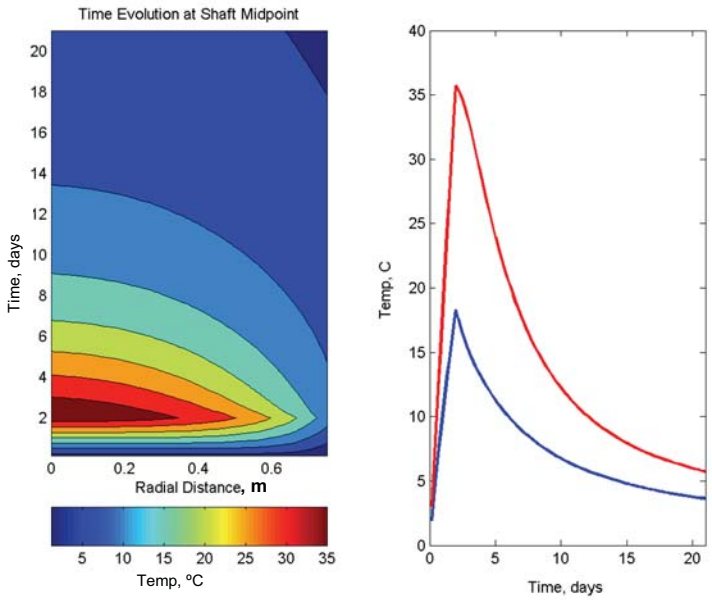

Figure 26. Chart. Thermal Evolution of Nominal Drilled Shaft. Maximum Temperature Increase ~35ºC, Mean Temperature Increase ~18ºC, Temperatures in Excess of Maxima (Peak) in Sample Persist for > 3 Weeks.

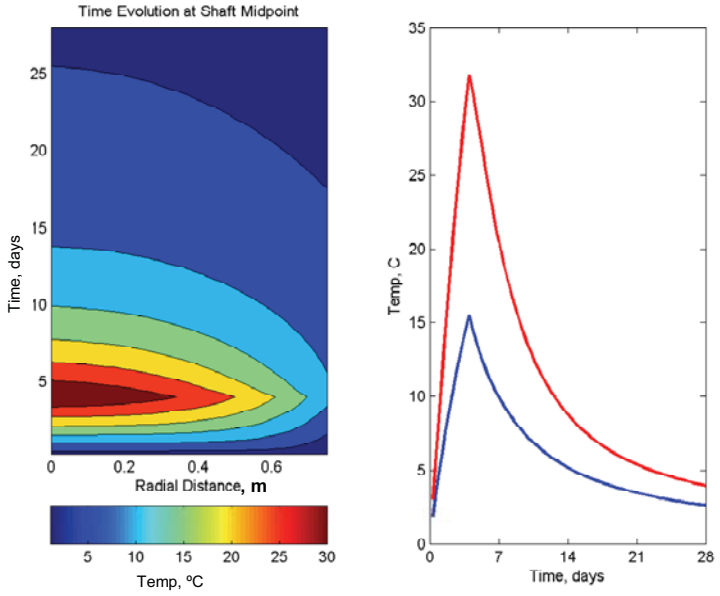

Figure 27. Chart. Thermal Evolution of Nominal Shaft with Curing Retarded by a Factor of 2 (End of First Phase of Curing at 4 Days, with Commensurate Decrease in Heating Rate). Peak Temperatures are Reduced only Slightly because Thermal Response Time of Shaft is still Comparable to Curing Time.

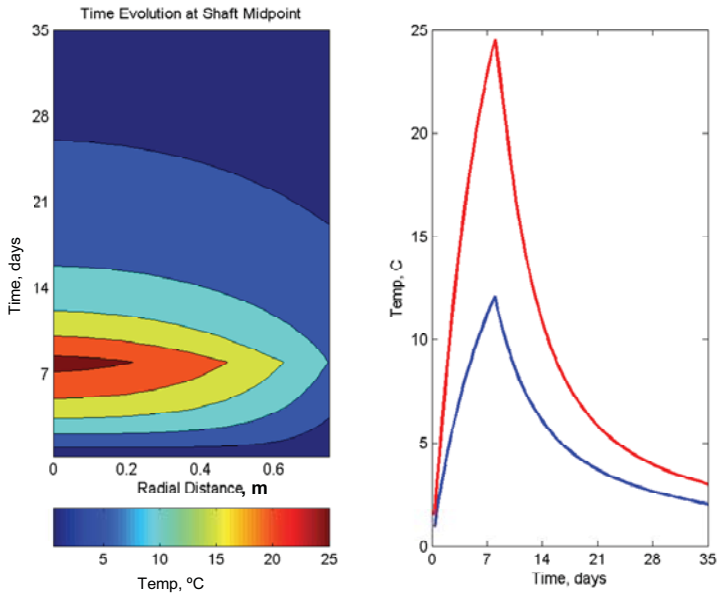

Figure 28. Chart. Thermal Evolution of Nominal Shaft with Curing Retarded by a Factor of 4. Peak Temperatures now Begin to Show Significant Reduction because Shaft Thermal Response Time (a Few Days) is Noticeably Smaller than Primary Curing Period (8 Days). Temperatures in excess of Sample Maxima are Relatively Unaffected, still Remaining High for >3 Weeks.

4.4 CONTINUOUS FIELD MONITORING OF DRILLED SHAFT FOUNDATIONS FOR CHANGES IN TEMPERATURE, VELOCITY, DENSITY, AND MOISTURE

In order to understand the mechanism by which a typical drilled shaft foundation cures under field conditions, two (2) shafts were monitored for up to seven (7) days using four (4) geophysical logging methods at the Hagerman National Wildlife Refuge near Sherman, Texas. The geophysical logging methods used included: 1) temperature logging to monitor changes in shaft's temperature; 2) crosshole sonic logging (CSL) to monitor changes in velocity; 3) gamma-gamma density logging (GDL) to monitor changes in density; and, 4) neutron-moisture logging (NML) to monitor changes in moisture.

4.4.1 Temperature Monitoring Results

Temperature monitoring was performed on two shafts at the Hagerman National Wildlife Refuge using both temperature logging and embedded thermocouples. In addition, one drilled shaft was monitored at the Sevenmile-Gooseberry Project, near Salina, Utah using only thermocouples.

4.4.1.1 *Temperature Monitoring Using Geophysical Temperature Logging*

Two (2) drilled shafts were continuously monitored using temperature logging method at the Hagerman National Wildlife Refuge, TX. These shafts were 0.9-1 m (3-3.5 ft) in diameter, between 13-14.5 m (42.5-47.5 ft) in depth, and were built as part of Harris Creek Bridge Project by the Federal Highway Administration-Central Federal Lands Highway Division. The two-span bridge contained two (2) abutments and one (1) pier line with two (2) shafts per substructure unit. Each shaft contained four 5-cm (2-in) Inside Diameter (I.D.) steel access tubes. Temperature logging was performed at Abutment 1, Shaft 1 and Pier 2, Shaft 2. Thermocouples were also installed in Abutment 2, Shaft 2 to monitor temperature of concrete continuously between August 31 to September 7, 2004. Class A (AE) concrete with required 28-day breaking strength of 27,600 kPa (4,000 psi) placement slump of 25-100 mm (1-4 inch), water/cement ratio of 0.44 (by weight) and air content of 5% was used to construct the drilled shaft.

Abutment 1, Shaft 1

Figure 29 displays the temperature monitoring results from Abutment 1 Shaft 1. The plots show temperature at 6 hours (shown in black), 12 hours (blue), and 24 hours (red) after the concrete placement. An initial rise in the shaft's temperature is observed in the first 24 hours after the concrete placement. In this figure, the temperature logs from four access tubes in the shaft are displayed as a function of depth on the vertical axis. Also presented in the depth axis is the soil profile as reported by the boring logs. The soil profile consisted of a gravel/boulders bed on the top 0.2 m (0.8 ft) followed by sand (mixed with clay) to 6.7 m (22 ft) depth, clay (mixed with sand) to 14 m (46 ft) depth, overlying blue shale bedrock. Groundwater table was at 3.8 m (12.5 ft) depth.

In Figure 30, the temperature logs from the first 24 hours after the concrete placement were combined with other temperature logs from two to six days indicating a gradual decrease in

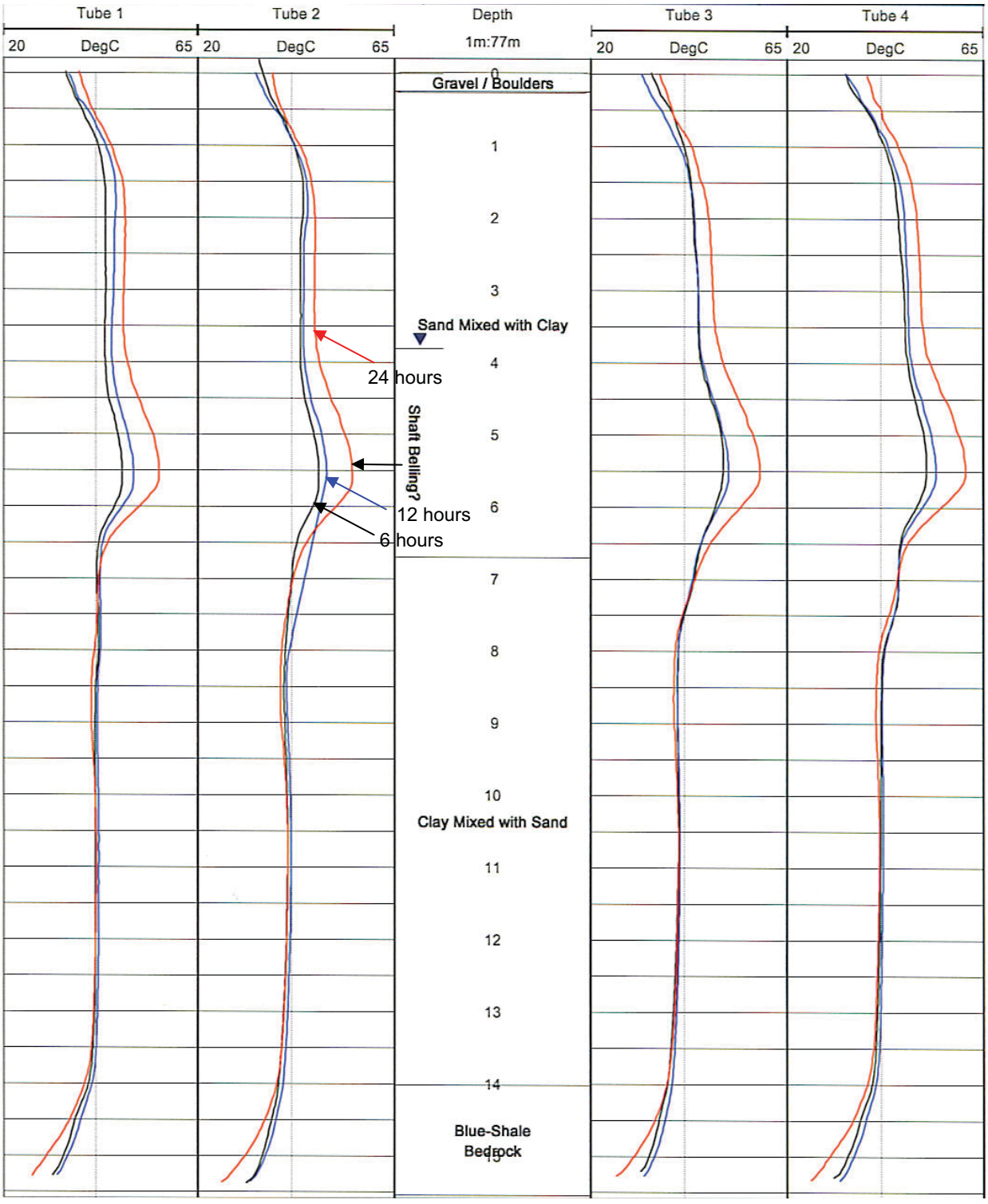

Figure 29. Plot. Temperature Monitoring of Abutment 1 Shaft 1. Hagerman National Wildlife Refuge, TX. Temperature Curves at 6 Hours (Black), 12 Hours (Blue) and 24 Hours (Red) After the Concrete Placement. Vertical Guideline: 41.5 ºC.

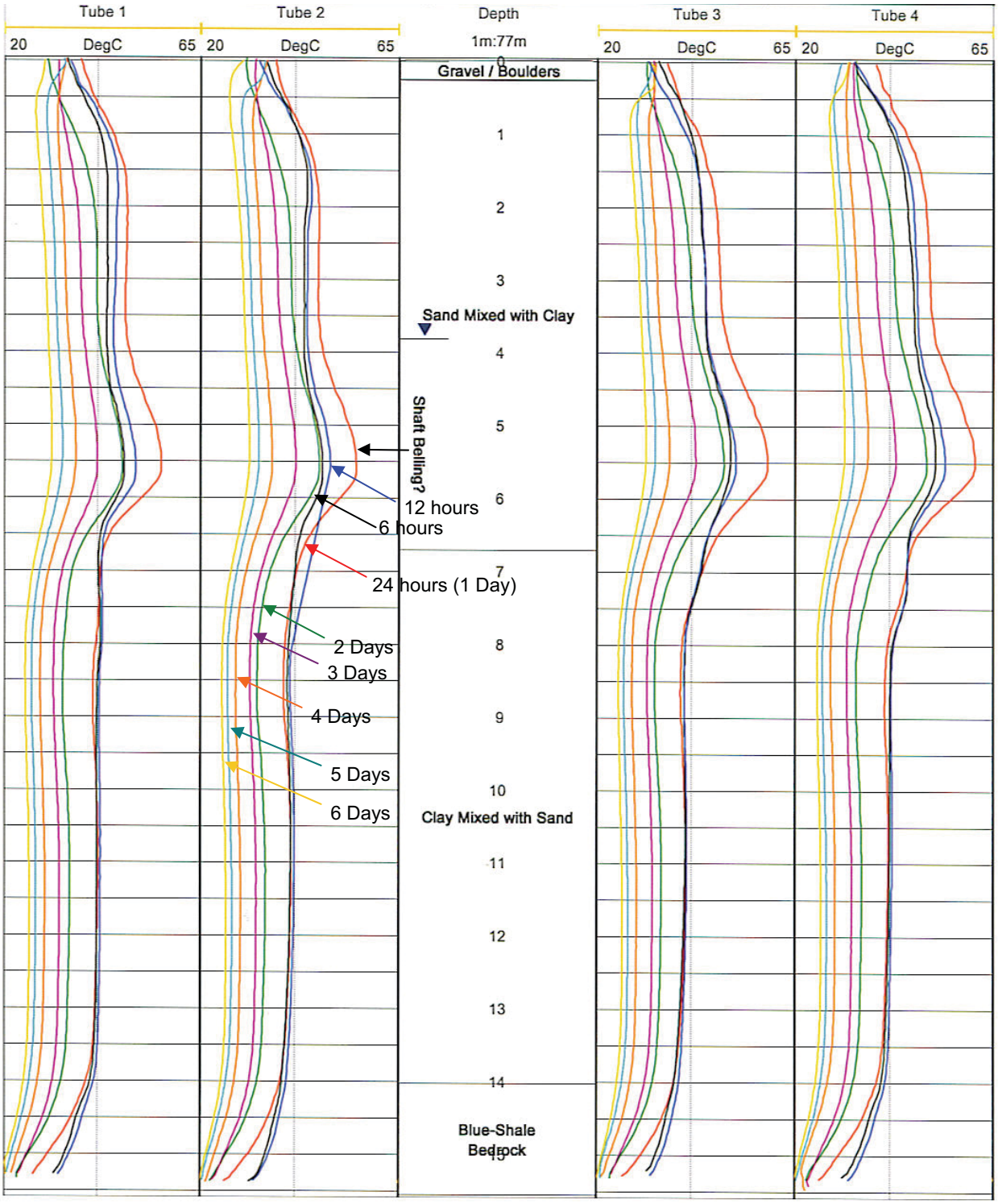

Figure 30. Plot. Temperature Monitoring of Abutment 1 Shaft 1. Hagerman National Wildlife Refuge, TX. Temperature Curves at 6 Hours (Black), 12 Hours (Blue), 24 Hours (1 Day, Red), 2 Days (Green), 3 Days (Purple), 4 Days (Orange), 5 Days (Teal), and 6 Days (Yellow) After the Concrete Placement. Vertical Guideline: 41.5 ºC.

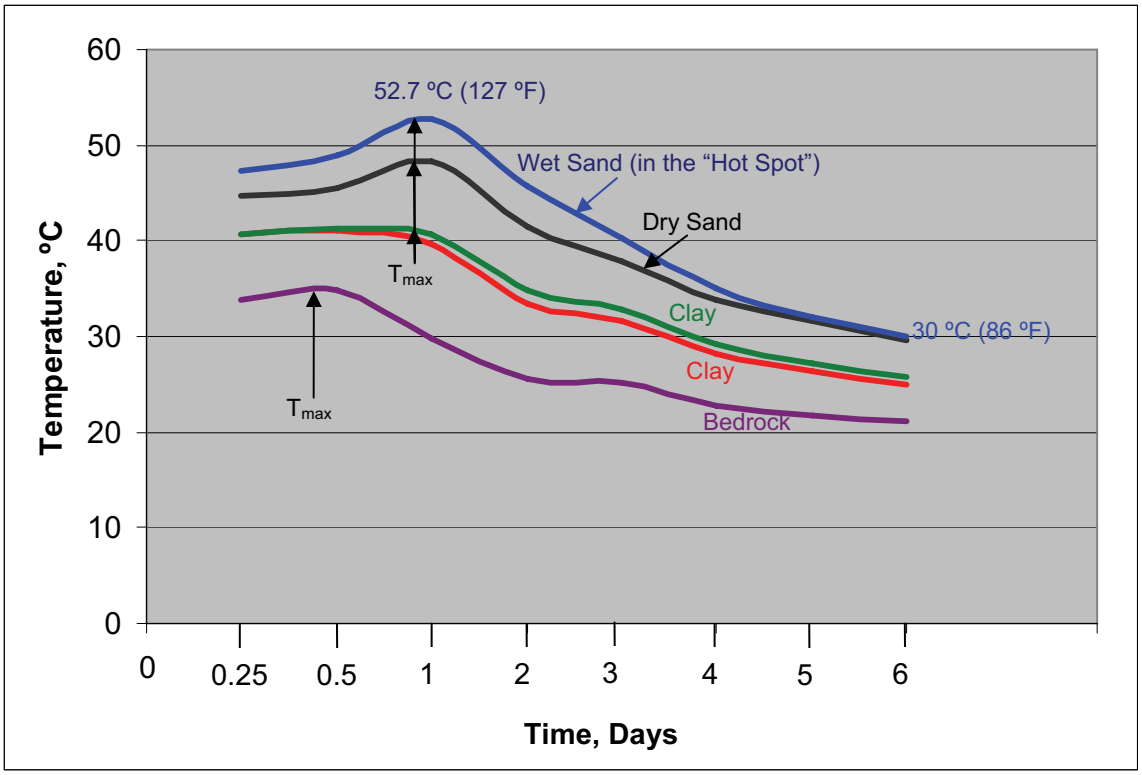

Figure 31. Graph. Temperature Monitoring of Abutment 1 Shaft 1. Hagerman National Wildlife Refuge, TX. Temperature Values are Averaged from the Four Access Tubes at 3m (Black), 6 m (Blue), 9 m (Red), 12 m (Green), and 15 m (Magenta) Depth Points.

temperature after the initial rise. Therefore, in this figure, the complete thermal history of the shaft in the first 6 days after the concrete placement is presented.

Finally, temperature values at five different depth points in Figure 30 are plotted as a function of time in Figure 31. In this figure, the temperature values from the four access tubes are averaged at 3m (in sand above the groundwater table displayed in black); at 6 m (in sand below the groundwater table in blue); at 9 m (clay in red); at 12 m (clay in green); and at 15 m (bed rock in magenta) levels.

The following conclusions can be drawn from the temperature logging studies from this shaft:

1. At a given time period after the concrete placement, the shape of the temperature curve appears to be a function of the thermal conductivity of the soil/rock at the hole. Therefore, in a typical drilled shaft, the shaft's temperature, and its curing rate or age, is non-uniform with depth. In our example, the shaft's temperature was highest (least cure) in the sand/gravel zones, cooler in the clayey zone, and coolest (most cure) at the bedrock level.
2. In the sandy zone, shaft's temperature rises more rapidly than at the clay and bedrock levels. From Figure 31, it is evident that peak temperature was reached about 12 hours after the concrete placement in the clay and bedrock levels as compared to 24 hours in the sand level. Peak temperatures were reached after 12 hours at 9 m, 12 m, and 15 m depths and after 24 hours at 3m and 6 m depths. The maximum temperature reached

was at 52.7 ºC (127 ºF) (at 6 m depth) which was reduced to 30 ºC (86 ºF) after 6 days. Maximum temperature differential in the shaft after 1 day of curing was about 23 ºC (41 ºF). This differential was reduced to 9 ºC (16 ºF) after 6 days of curing making the temperature curve more uniform in shape (compare the shape of the yellow curve (6 days old) to the red curve (1 day old) in Figure 30).

3. A localized "hot spot" was observed in Abutment 1 Shaft 1 as shown in Figures 29 and 30 between the depths of 3.7-7.7 m (12-25 ft). According to the construction records, an additional 6-7.5 m^3 (8-10 $yard^3$) of concrete had to be used at these depths. Therefore, it appears that the higher temperatures can be due to shaft belling at these depths.
4. Near the surface, in the top 1 m (3.3 ft) cooler temperatures were observed due to heat escaping to the air. For Tubes 2 and 3, shaft's temperature actually decreased between 6 to 12 hours before rising in 24 hours (Figure 29). After 24 hours, the temperature decreased except in the top 0.6 m (2 ft) which started to increase again after 3 days (Figure 30). Therefore, high fluctuation in temperature was observed in top 0.6 m (2 ft) of the shaft.

Pier 2, Shaft 2

A second set of temperature monitoring study was conducted in Pier 2, Shaft 2. The results are shown in Figure 32 from 1 hour to 6 days after the concrete placement. The soil profile consisted of a peat gravel on the top 1.22 m (4 ft) followed by clay with organics to 2.3 m (7.5 ft) depth, clay to 11.28 m (37 ft) depth, overlying a blue shale bedrock. Groundwater table was at the ground surface.

In Figure 33, temperature values at five different depth points are plotted as a function of time. In this figure, the temperature values from the four access tubes are averaged at 0.8 m (in gravel displayed in black); at 5 m (in clay in blue); at 10 m (clay in red); and at 12.5 m (shale bedrock in green).

The following conclusions can be drawn from the temperature logging studies from this shaft:

1. At a given time period after the concrete placement, the shape of the temperature curve appears to be a function of the thermal conductivity of the soil/rock at the hole. The shaft's temperature was highest (least cure) in the clay zone, cooler near the surface, and coolest (most cure) in the bedrock. No localized "hot spot" was observed in this dataset.
2. From Figure 33, it is evident that peak temperatures were reached after 24 hours. The maximum temperature reached was at 53 ºC (127 ºF) (at 5 m depth) which was reduced to 35 ºC (95 ºF) after 5 days. Maximum temperature differential in the shaft (at different depth levels) was about 10 ºC (18 ºF) after 6 hours (0.04 days) of curing. This differential was reduced to 3.7 ºC (6.6 ºF) after 5 days of curing making the temperature curve more uniform in shape (compare the shape of the teal curve (5 days old) to the black curve (1 hour old) in Figure 32).
3. Near the surface, in the top 1 m (3.3 ft) cooler temperatures were observed due to heat escaping to the air.

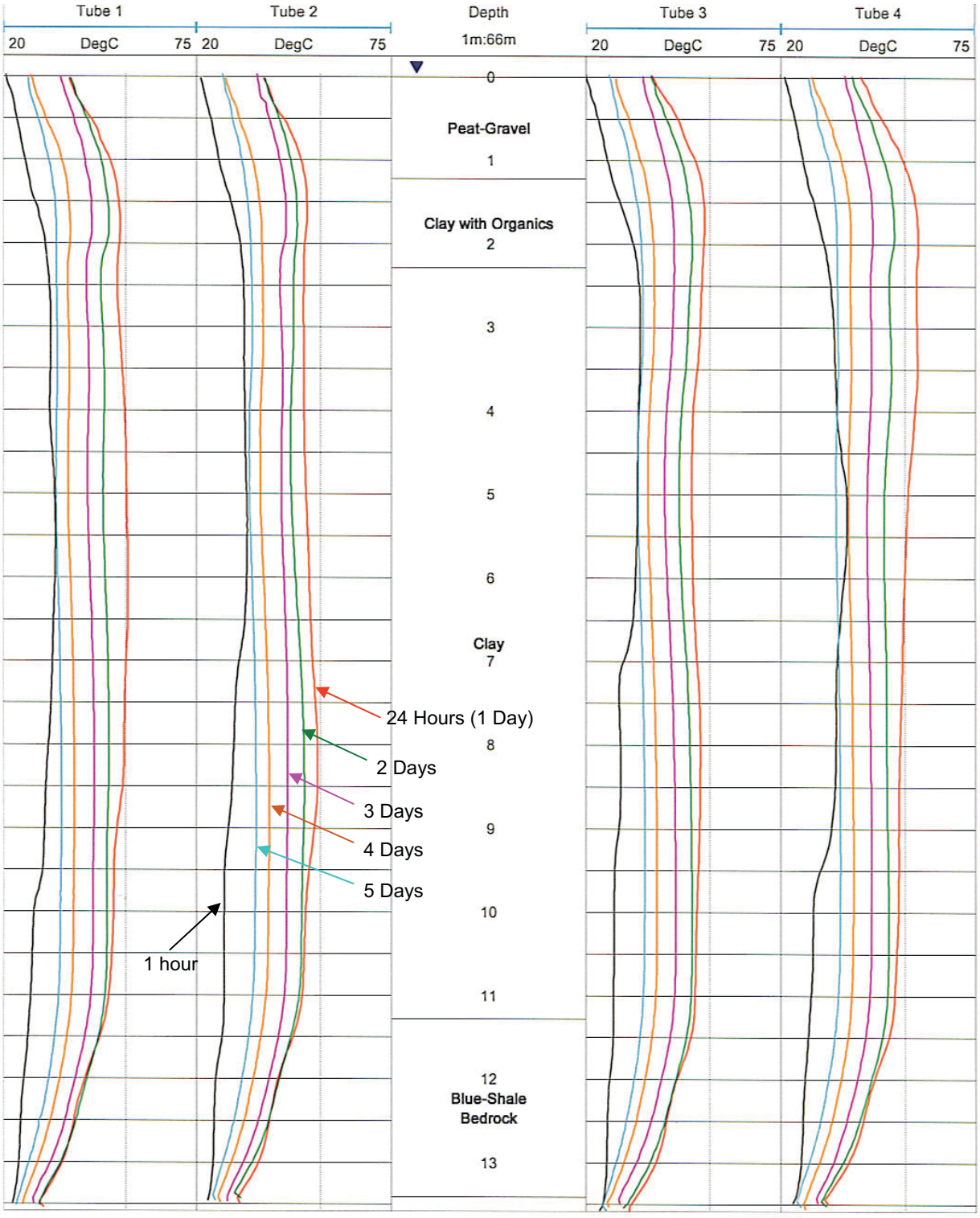

Figure 32. Plot. Temperature Monitoring of Pier 2 Shaft 2. Hagerman National Wildlife Refuge, TX. Temperature Curves at 1 Hour (Black), 24 Hours (1 Day, Red), 2 Days (Green), 3 Days (Purple), 4 Days (Orange), and 5 Days (Teal) After the Concrete Placement. Vertical Guideline: 55 ºC.

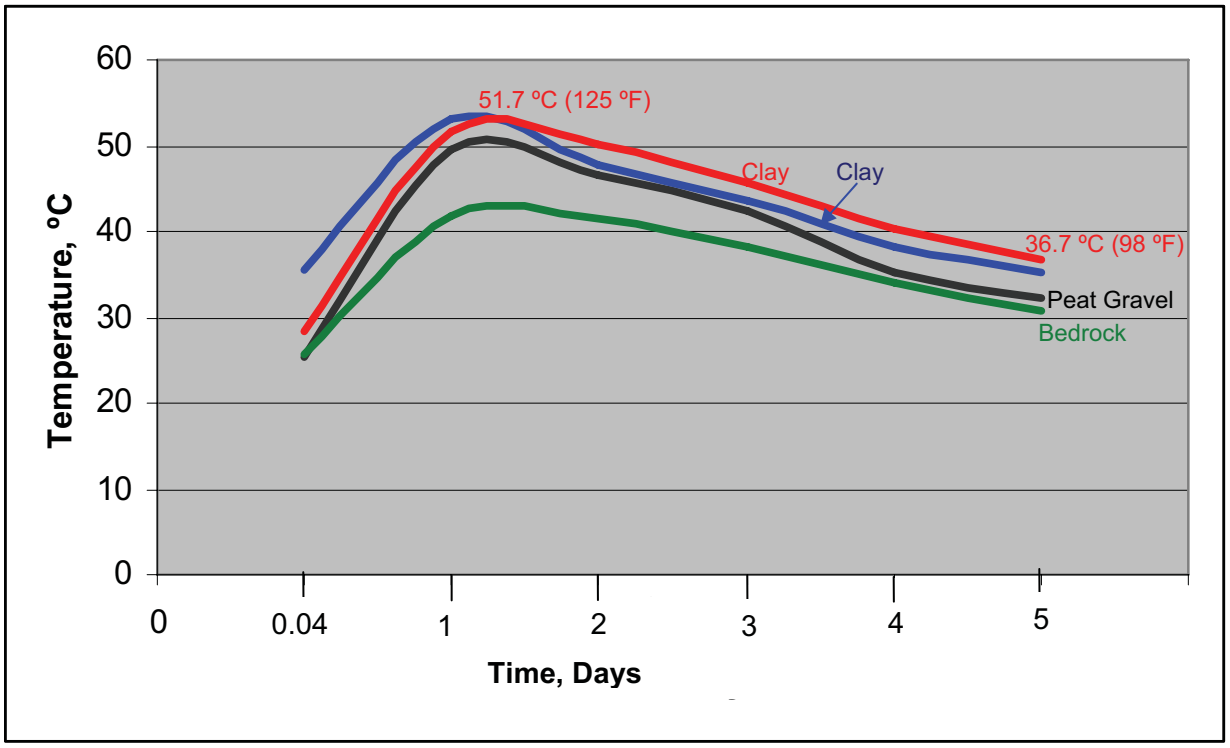

Figure 33. Graph. Temperature Monitoring of Pier 2 Shaft 2. Hagerman National Wildlife Refuge, TX. Temperature Values are Averaged from the Four Access Tubes at 0.8m (Black, Gravel), 5 m (Blue, Clay), 10 m (Red, Clay), and 12.5 m (Green, Shale Bedrock) Depth Points.

4.4.1.2 *Temperature Monitoring Using Embedded Thermocouples*

Embedded thermocouples were used in order to monitor shaft's temperature at two sites, as is described next.

I. Hagerman National Wildlife Refuge Project.

At the Hagerman National Wildlife Refuge Project, a third shaft—Abutment 2, Shaft 2, was monitored with two thermocouples one installed at the *center* and the other attached to the rebar cage (*side*) at 2.4 m (8 ft) depth. The center thermocouple was attached to a single rebar that was pushed in the shaft immediately after the concrete placement. This study was performed to investigate the temperature differential between the center of the shaft and the side of the shaft at the rebar cage level.

As shown in Figure 34, peak temperature was reached after 26 hours both at the center and at the rebar cage in the shaft. The maximum temperature reached was at 68.3 ºC (155 ºF) at the center and 66.1 º C (151 ºF) at the cage. Maximum temperature differential between the center and the side was recorded at 5 ºC (9 ºF) after 29 hours after concrete placement.

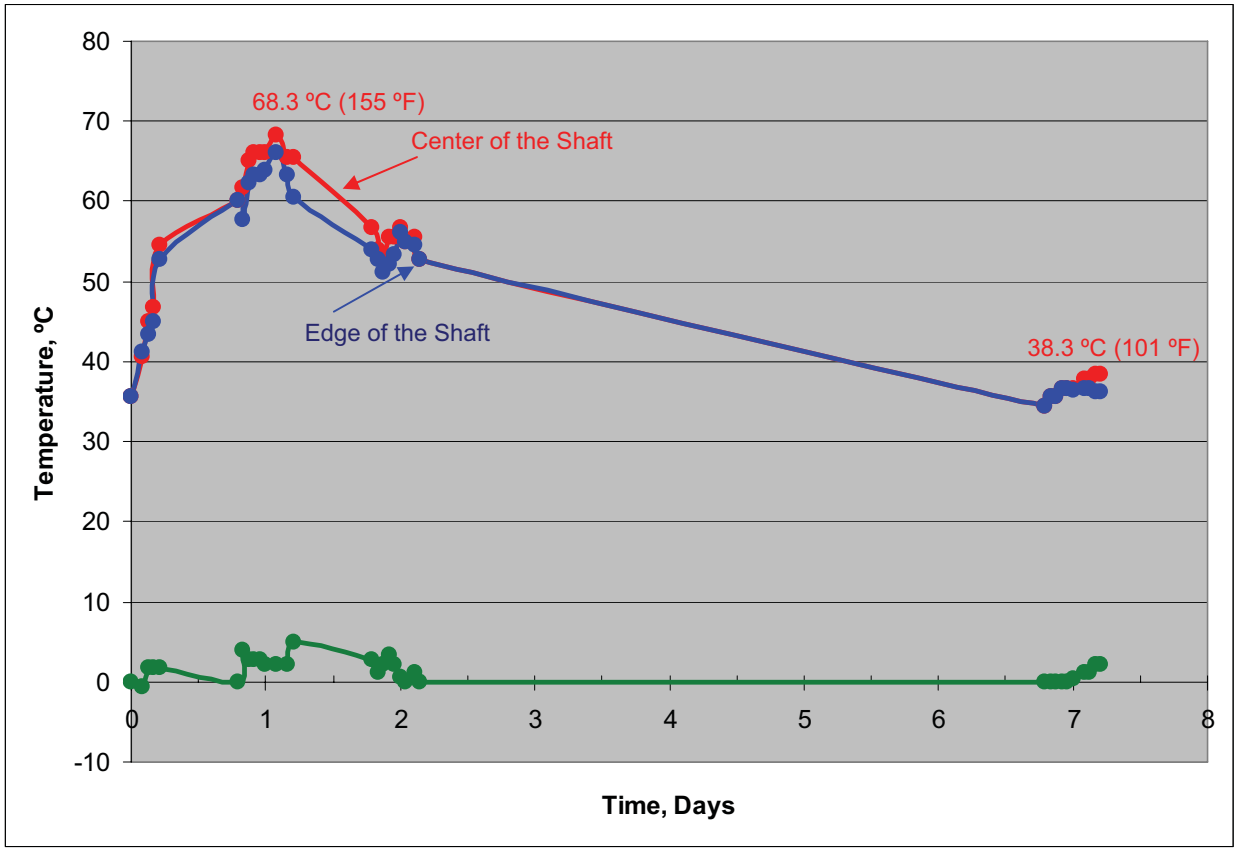

Figure 34. Graph. Temperature Monitoring of Abutment 2 Shaft 2 Using Embedded Thermocouples. The Red Curve Displays the Temperature Readings at the Center of the Shaft at 2.4 m (8 ft), Blue Curve Displays Temperature Reading Near the Rebar Cage at the Same Depth, and the Green Curve Displays the Temperature Differential Between the Two Stations. Hagerman National Wildlife Refuge, TX.

II. Sevenmile-Gooseberry Road Project

At another project, drilled shaft P-3 from the Sevenmile-Gooseberry Road CFLHD Project near Salina, Utah was continuously monitored for a period of 18 days with results shown in Figure 35. Two thermocouple probes were installed outside the rebar cage in approximately two o'clock position (with twelve o' clock representing North) at 3.66 m (12 ft, shown in red) and 12.8 m (42 ft shown in blue) depths. Since the groundwater table was 8.23 m (27 ft), the two probes were located at 4.57 m (15 ft) above and below the groundwater table.

Class A 19-cm (7.5-inch) slump concrete with 6.0% air was used. The concrete temperature at the delivery was 11.1 ºC (52 ºF). Concrete was placed on May 15, 2004 at 12:30 p.m. and the concrete placement was completed at 2 p.m., where the first temperature readings were taken.

As shown in Figure 35, peak temperature was reached after about 20 hours at 41 ºC (106 ºF).

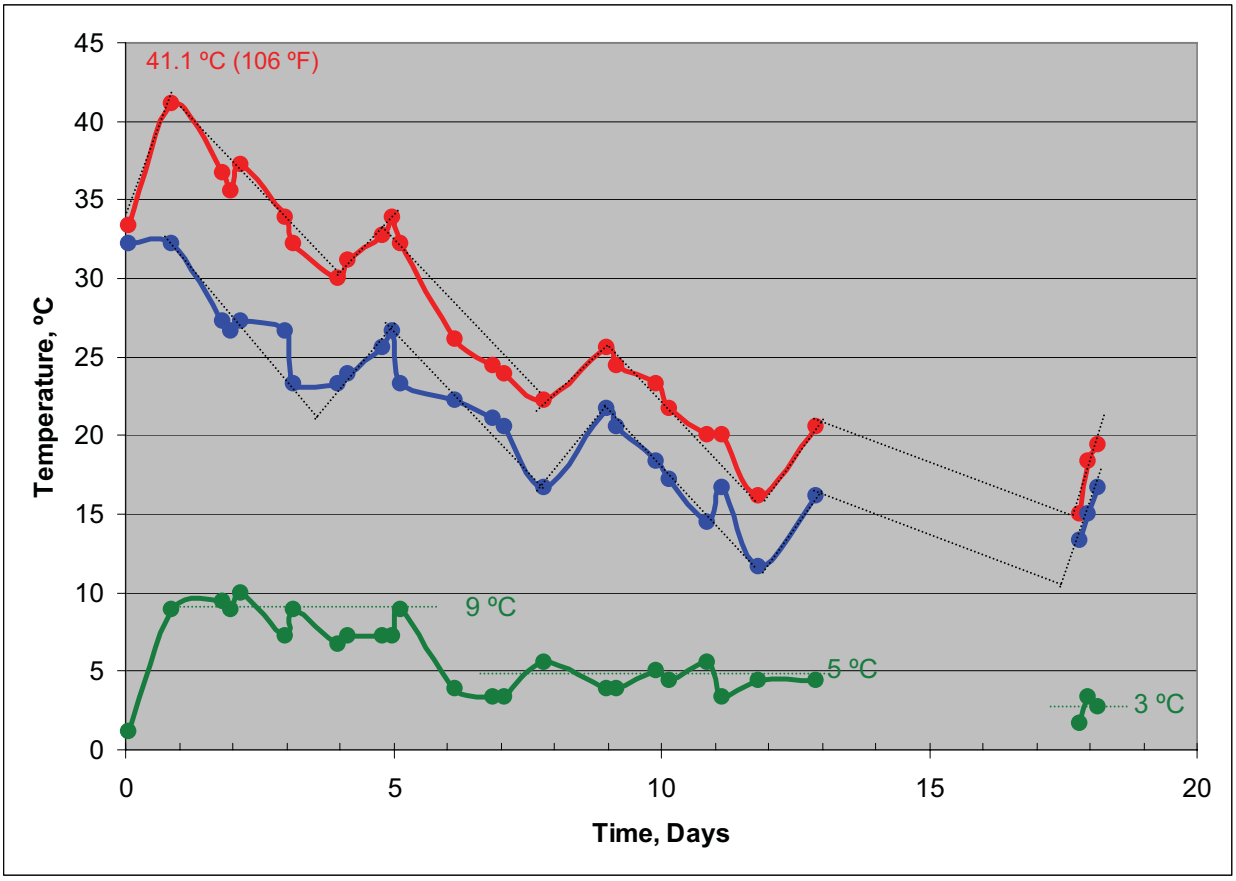

Figure 35. Plot. Temperature Monitoring of Shaft P-3 Using Embedded Thermocouples Near the Rebar Cage. The Red Curve Displays the Temperature Readings at 3.66 m (12 ft) (Above the Groundwater Table), Blue Curve at 12.8 m (42 ft) (Below the Groundwater Table), and the Green Curve Displays the Temperature Differential Between the Two Stations. Gooseberry-Sevenmile Project, UT.

The following conclusions can be drawn from this study:

1. At both measurement depths, the temperature curves are similar in shape and both decrease with time as the shaft is loosing heat as the result of heat of hydration.
2. The shaft temperature measurements at the rebar cage are not uniform with depth. As expected, the groundwater table acted as a heat sink with the thermocouple placed at 4.57 m (15 ft) below the groundwater table measuring lower average temperatures than the one placed at 4.57 m (15 ft) above the groundwater table. Therefore, the shaft is generally hotter (less cured) above the groundwater table.
3. Interestingly, at each measurement location, the temperature curve seems to recover and display distinct temperature jumps at about 4-day intervals.
4. The temperature differential between the two stations decreased with time as the shaft's temperature (or curing rate) becomes more uniform with time. The temperature difference at the two stations is about 9 ºC (16ºF) for the first 1-5 days, decreasing to

about 5ºC (9 ºF) for the next 7 days, and to about 3 ºC (5.4 ºF) after 18 days of measurement.

4.4.1.3 *Conclusions — Temperature Monitoring Studies*

From both the temperature logging and embedded thermocouples studies, the following can be concluded:

- For the small diameter shafts under this study (less than 1 m (3.5 ft) in diameter), peak temperatures of about 41-68 ºC (106-154 ºF) were reached between 12- 26 hours after concrete placement.
- The peak temperatures were reduced to about 23-35 ºC (73-95 ºF) after 6 days and about 12 ºC (54 ºF) after 12 days following concrete placement.
- Shaft's curing rate (or age) is non-uniform as a function of depth in the first 6-7 days. It depends on shaft's diameter, soil properties at the hole, and groundwater table depth.
- After 6-7 days the shafts' temperature curve (and age) appear to reach a more uniform in shape with temperature differential of less than 5ºC (9 ºF) throughout.
- Therefore, if the CSL measurements (or tomographic imaging) are performed before the first 7 days of concrete placement, the sonic velocities (as it relates to concrete strength) will be lower than the lab measurements and non-uniform with depth, unless the concrete strength are based on maturity calculations.
- Temperature logging can be used to observe relative changes in thermal conductivity and possibly infer general soil properties.
- Temperature logging may also be used to detect shaft belling.
- Temperature logging can be used to measure shaft's peak temperature and temperature differential between the center and the edge (with insertion of a thermocouple in the center). This data can be used to mitigate thermal cracking and durability problems in the shaft. According to Gajda and Vangeem (2002), in mass concrete "temperature limits are specified to seemingly arbitrary values of 57ºC (135ºF) for the maximum allowable concrete temperature and 19ºC (35ºF) for the maximum allowable temperature difference between the center and the surface of the mass concrete section". A study is warranted to define these parameters in a drilled shaft environment.

4.4.2 Velocity Monitoring Results

Figure 36 displays the velocity monitoring results from Abutment 1 Shaft 1 at the Hagerman National Wildlife Refuge, TX from 1 day to 6 days after the concrete placement. Six crosshole sonic logs (CSL) were acquired using 4 perimeter logs and 2 diagonal logs. In Figure 36, the static-corrected CSL results are plotted in 6 separate sub-plots from 6 different access-tube pair combinations as indicated on the top label. Depths were measured from the top of the shaft and are shown on the vertical axis. Also presented in the depth axis is the soil profile as reported by the boring logs. In Figure 37, the diagonal CSL Paths 1-3 and 2-4 are plotted in an expanded scale and in Figure 38, the CSL values from four access tubes are averaged at five different depth points and plotted as a function of time.

Unfortunately, large tube bending was observed in top 7.5 m (24.6 ft) of the shaft (particularly note Path 3-4). This made static correction more difficult to apply. Also, it appears that low velocity values were observed in the bottom 1 m (3.3 ft) of the shaft.

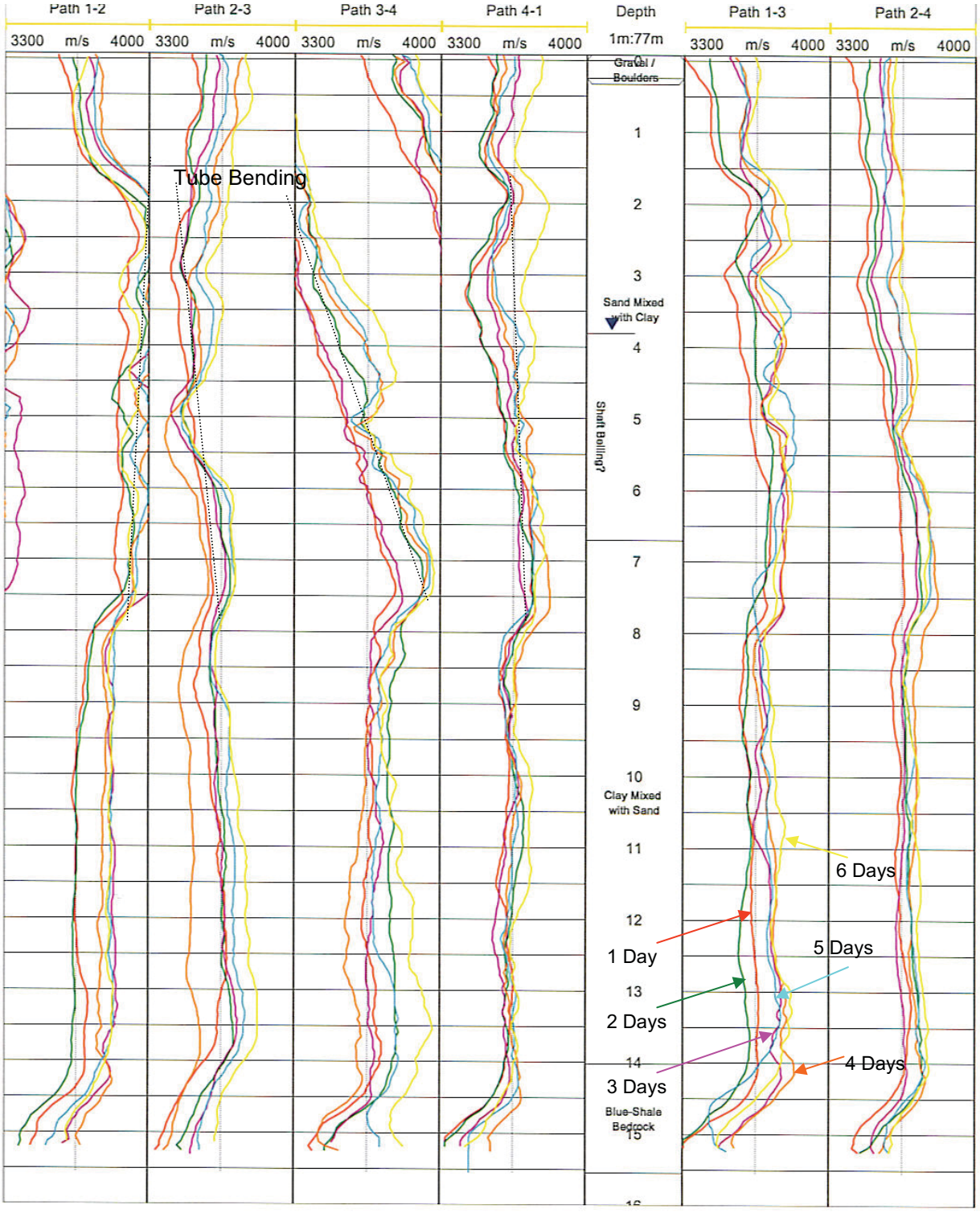

Figure 36. Plot. Velocity Monitoring of Abutment 1 Shaft 1. Hagerman National Wildlife Refuge, TX. CSL Velocity Curves at 1 Day (Red), 2 Days (Green), 3 Days (Purple), 4 Days (Orange), 5 Days (Teal), and 6 Days (Yellow) After the Concrete Placement. Vertical Guideline: 3,650 m/s.

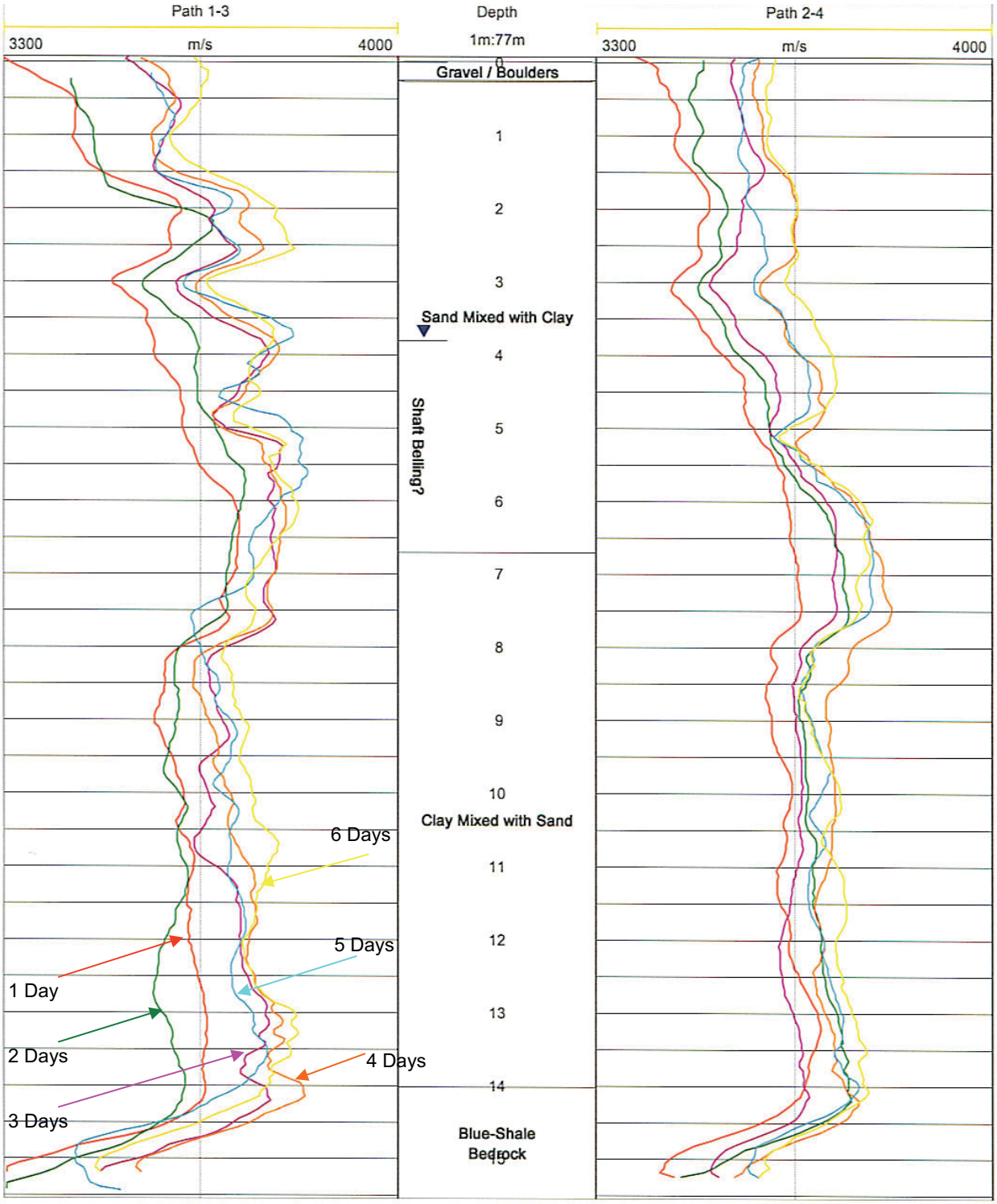

Figure 37. Plot. Velocity Monitoring of Abutment 1 Shaft 1. Hagerman National Wildlife Refuge, TX. CSL Velocity Curves from Tube Paths 1-3 and 2-4 at 1 Day (Red), 2 Days (Green), 3 Days (Purple), 4 Days (Orange), 5 Days (Teal), and 6 Days (Yellow) after Concrete Placement. Vertical Guideline: 3,650 m/s.

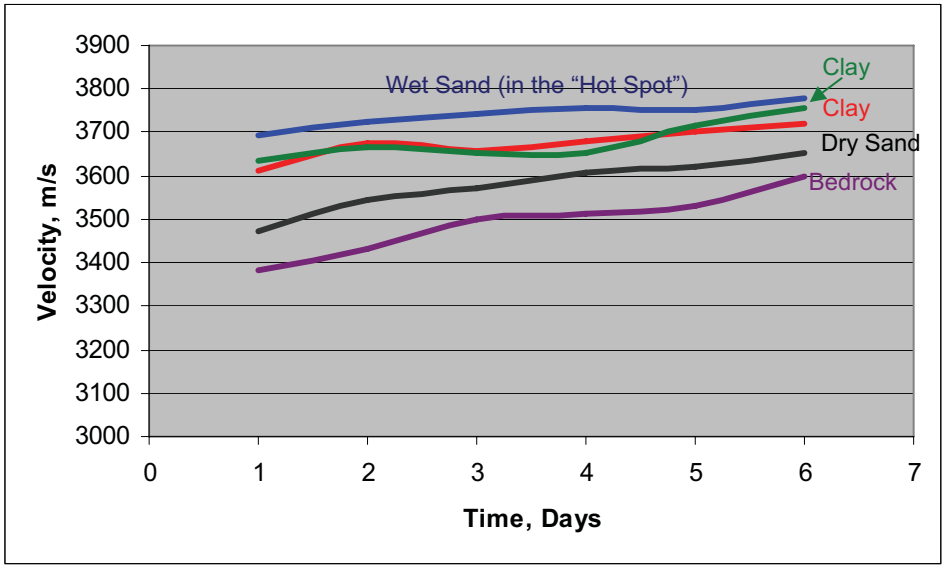

Figure 38. Graph. Velocity Monitoring of Abutment 1 Shaft 1. Hagerman National Wildlife Refuge, TX. Static Corrected Velocity Values are Averaged from the Four Access Tubes (and Six CSL Test Paths) at 3m (Black), 6 m (Blue), 9 m (Red), 12 m (Green), and 15 m (Magenta) Depth Points.

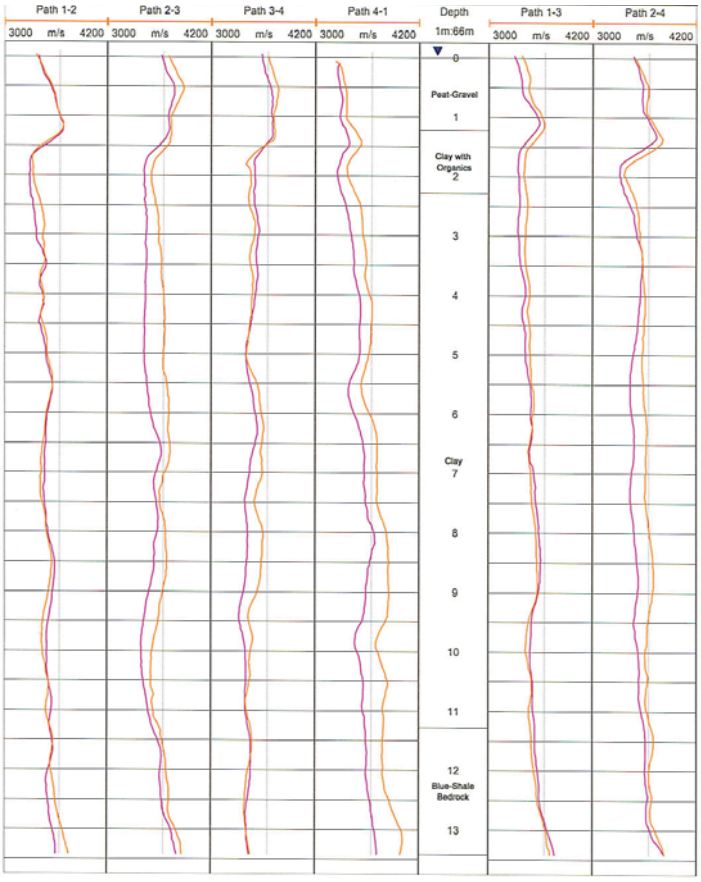

Figure 39. Plot. Velocity Monitoring of Pier 2 Shaft 2. Hagerman National Wildlife Refuge, TX. CSL Velocity Curves at 3 Days (Purple) and 4 Days (Orange) After the Concrete Placement. Vertical Guideline: 3,650 m/s.

Limited CSL monitoring was obtained from Pier 2 Shaft 2 from 3 days and 4 days after the concrete placement. As indicated in Figure 39, a small increase in CSL velocity is observed from 3 and 4 days after the concrete placement.

From this velocity monitoring study, the following conclusions can be drawn:

1. Velocity values appear to increase with time of curing. This well apparent for the Pier 2 Shaft 2 shown in Figure 39. For Abutment 1 Shaft 1 in Figure 36, the CSL curves on the whole were increasing with time; but not continuously. For the long CSL Paths 1-3 and 2-4 plotted in an expanded scale in Figure 37, the velocity increase was more apparent. However, when the CSL values from four access tubes are averaged at five different depth points in Figure 38, a clear increase in velocity is observed.
2. At a given time period, velocity values appear to inversely correlate with shaft's temperature. For Pier 2 Shaft 2, the velocity values in Figure 39 correlated well with the shaft's temperature shown in Figure 33 with clay indicating the lowest velocity (warmest), followed by gravel (cooler), and bedrock indicating highest velocity (coolest temperature). For Abutment 1 Shaft 1, average velocities should have increased from sand (warmest), followed by clay, and bedrock indicating highest velocity (coolest). This trend was generally observed; however, bedrock velocities were anomalously low (possibly due to a defect) and wet sand was anomalously high possibly due to being situated within the tube bending zone.
3. The velocity curves appears to taper off after about 4 days of curing.

4.4.3 Density Monitoring Results

Figure 40 displays the density monitoring results from Abutment 1 Shaft 1 at the Hagerman National Wildlife Refuge, TX from 1 day to 6 days after the concrete placement. In this figure, the GDL results are plotted in 4 separate sub-plots from the tested access tubes. Each individual sub-plot depicts the GDL results from 35.5 cm (14 in) source-detector separation presented in a magnified density scale of 130-200 lbs/ft^3 (2,100-3,200 kg/m^3). Depths were measured from the top of the shaft and are shown on the vertical axis. Also presented in the depth axis is the soil profile as reported by the boring logs. The single-hole GDL results were more uniform than the CSL results as they are not affected by tube bending. In Figure 41, GDL values from four access tubes are averaged at five different depth points and plotted as a function of time.

GDL monitoring was obtained from Pier 2 Shaft 2 from 1 day to 4 days after the concrete placement. As indicated in Figure 42, a steady increase in density values are observed in this dataset.

From this density monitoring study, the following conclusions can be drawn:

1. Density values appear to slightly increase with time of curing. This is well apparent for the Pier 2 Shaft 2 shown in Figure 42 for 1 to 4 days of curing. For Abutment 1 Shaft 1 in Figure 40, the density values also increased steadily from 1 to 4 days after the concrete placement. However, values then decreased after days 5 and 6. The reason is unclear—possibly due to the formation of voids at this time. This decrease in density values are

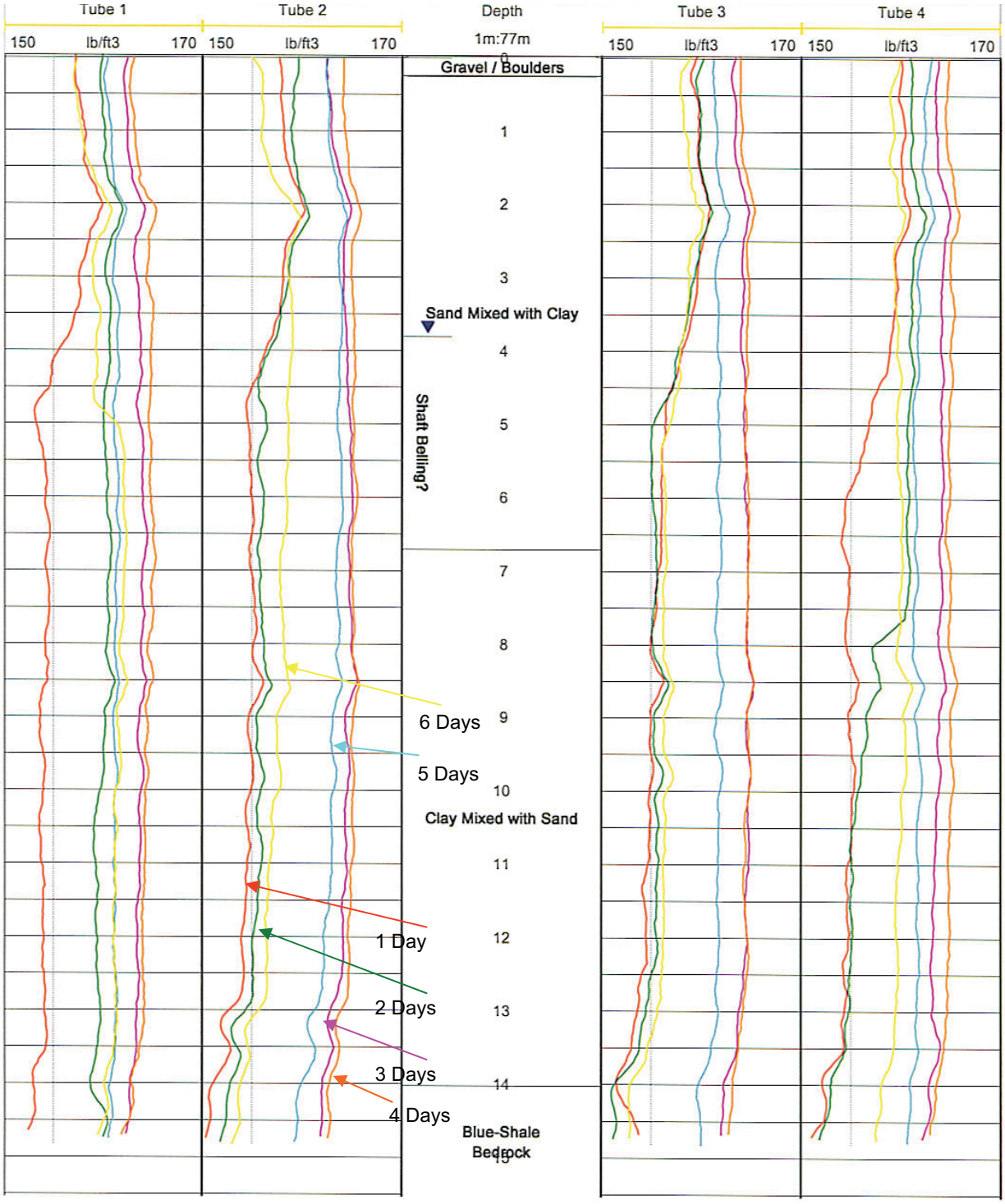

Figure 40. Plot. Density Monitoring of Abutment 1 Shaft 1. Hagerman National Wildlife Refuge, TX. GDL Density Curves with 1 Day (Red), 2 Days (Green), 3 Days (Purple), 4 Days (Orange), 5 Days (Teal), and 6 Days (Yellow) After the Concrete Placement. Vertical Guideline: 155 lb/ft^3.

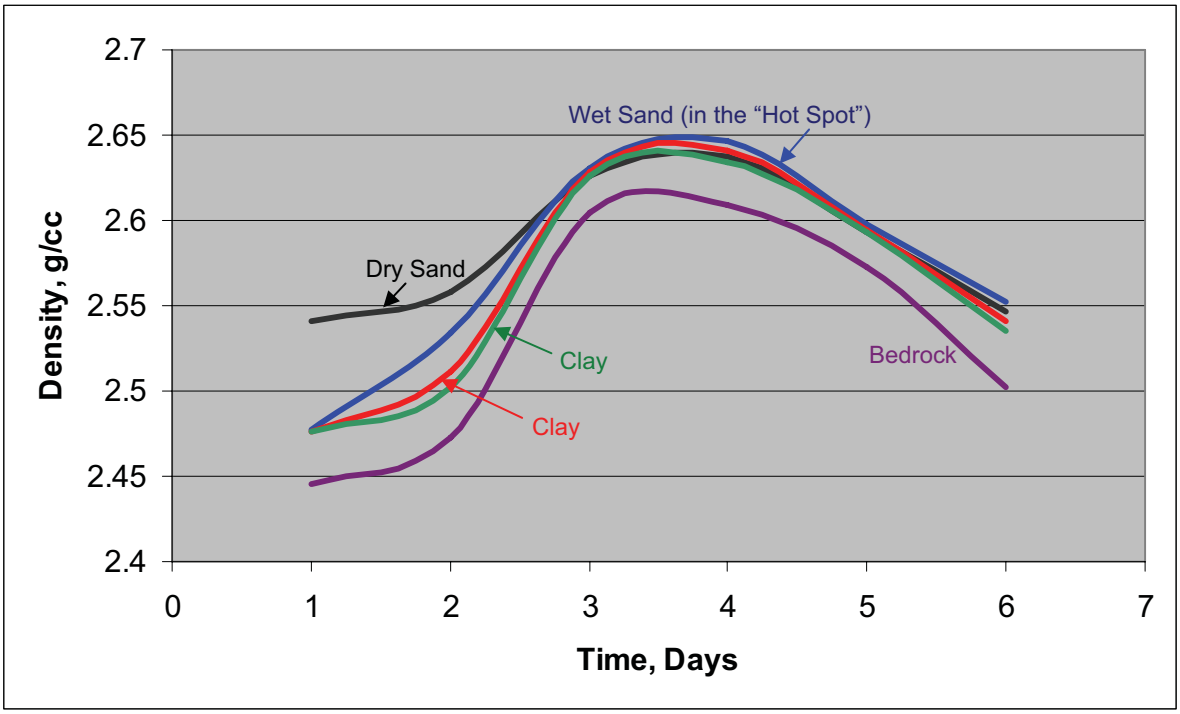

Figure 41. Graph. Density Monitoring of Abutment 1 Shaft 1. Hagerman National Wildlife Refuge, TX. Density Values are Averaged from the Four Access Tubes at 3m (Black), 6 m (Blue), 9 m (Red), 12 m (Green), and 15 m (Magenta) Depth Points.

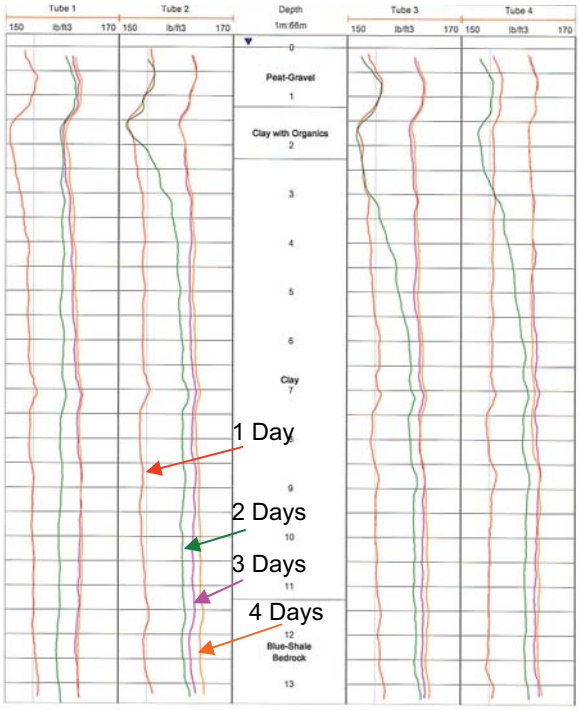

Figure 42. Plot. Density Monitoring of Pier 2 Shaft 2. Hagerman National Wildlife Refuge, TX. GDL Density Curves at 1 Day (Red), 2 Days (Green), 3 Days (Purple), and 4 Days (Orange) After the Concrete Placement. Vertical Guideline: 155 lb/ft^3.

also demonstrated in Figure 41. In this figure, the averaged GDL values are plotted from 3m (in sand above the groundwater table displayed in black); 6 m (in sand below the groundwater table in blue); 9 m (clay in red); 12 m (clay in green); and 15 m (bed rock in magenta) depth levels.

2. At a given time period, the shape of the density (GDL) curves appear to correlate with moisture (NML) curves (Section 4.4.4). For Pier 2 Shaft 2, the density values in Figure 42 correlated well with the shaft's relative moisture levels shown in Figure 45 with gravel (lowest moisture, lowest density), followed by clay and bedrock (highest moisture, highest density). For Abutment 1 Shaft 1, however, an inverse correlation was observed—possibly due to anomalously low densities in the bedrock (due to a probable "defect") and anomalously high densities in the sand (possibly due to erroneous reading in the "hot spot" zone).

4.4.4 Moisture Monitoring Results

Figure 43 displays the neutron monitoring logging (NML) results from Abutment 1 Shaft 1 at the Hagerman National Wildlife Refuge, TX from 1 day to 6 days after the concrete placement. In this figure, the NML results are plotted in 4 separate sub-plots from the tested access tubes. Each individual sub-plot is presented in a magnified scale of 90-170 counts per second (cps). Lower counts denote higher moisture content; therefore, in each sub-plot, moisture content increases from left to right. Depths were measured from the top of the shaft and are shown on the vertical axis. Also presented in the depth axis is the soil profile as reported by the boring logs. In Figure 44, NML values from four access tubes are averaged at five different depth points and plotted as a function of time. A more limited NML monitoring was obtained from Pier 2 Shaft 2 from 2 days to 4 days after the concrete placement and is displayed in Figure 45.

From this neutron-moisture monitoring study, the following conclusions can be drawn:

1. Relatively speaking, the moisture level in Abutment 1 Shaft 1 in Figure 43 was highest at the bedrock followed by clay and sand (lowest). Therefore, for the initial "green" concrete, it appears that the less permeable clay and shale layers allowed less movement of moisture out of the concrete matrix. This trend is also well demonstrated in Figure 44 where the averaged NML values are plotted from 3m (in sand above the groundwater table in black); 6 m (in sand below the groundwater table in blue); 9 m (clay in red); 12 m (clay in green); and 15 m (bedrock in magenta). Similar results were observed in the NML data from Pier 2 Shaft 2 (Figure 45).
2. After 24 hours, moisture values appear to change negligibly with time of curing.

4.4.5 Summary of the Geophysical Monitoring Study

In summary, it appears that the curing strength of the concrete in a drilled shaft is not only a function of time but also a function of the physical properties of the surrounding soil/rock and the depth of the groundwater table. Specifically, two parameters from the soil profile that is noteworthy: thermal conductivity and permeability. Conductivity controls relative changes in temperature and permeability controls small relative changes in the moisture content. These parameters in turn control curing (age) and concrete strength—as it relates to incremental changes in velocity and density.

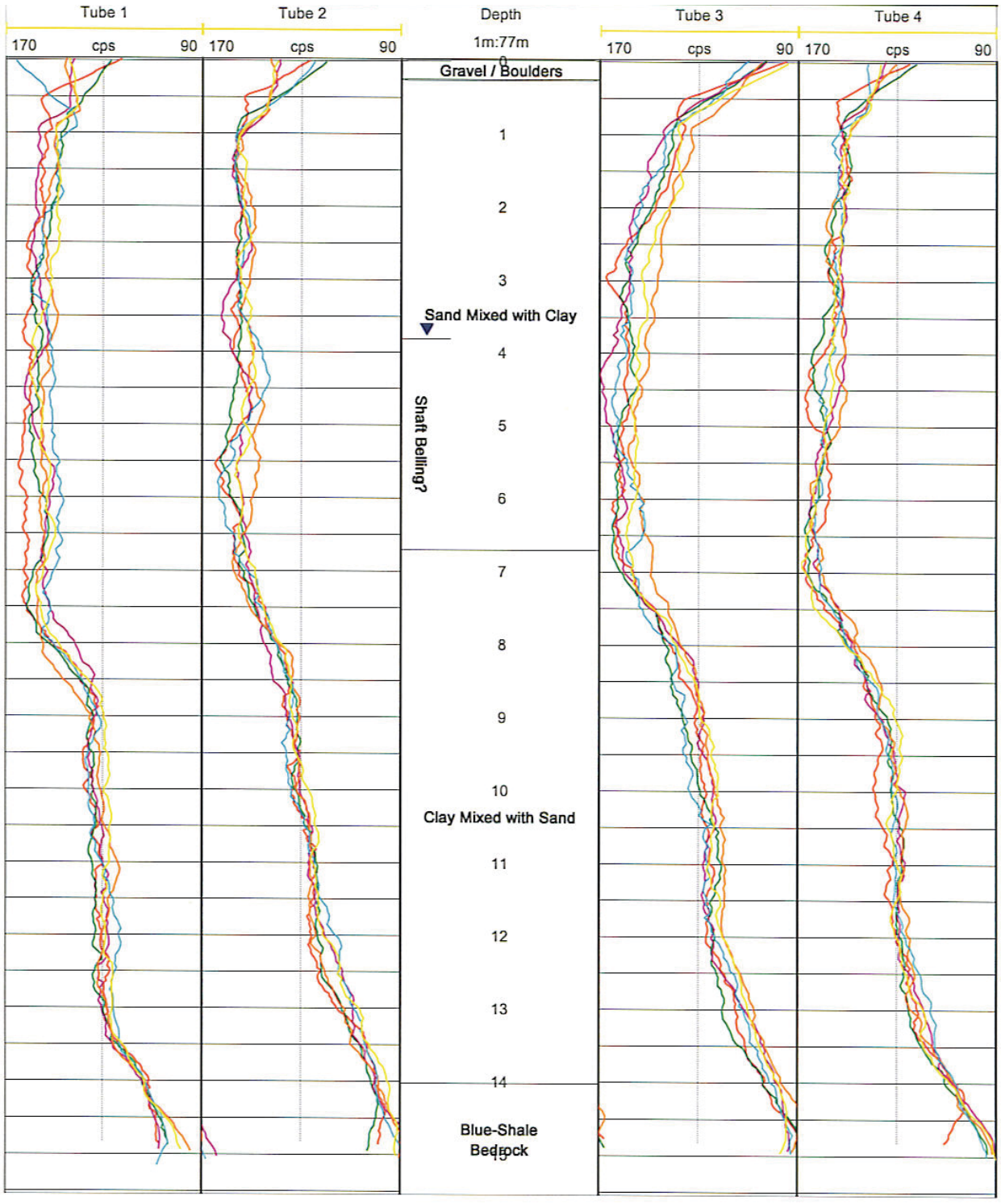

Figure 43. Plot. Moisture Monitoring of Abutment 1 Shaft 1. Hagerman National Wildlife Refuge, TX. NML Moisture Curves at 1 Day (Red), 2 Days (Green), 3 Days (Purple), 4 Days (Orange), 5 Days (Teal), and 6 Days (Yellow) After the Concrete Placement. Vertical Guideline: 130 cps.

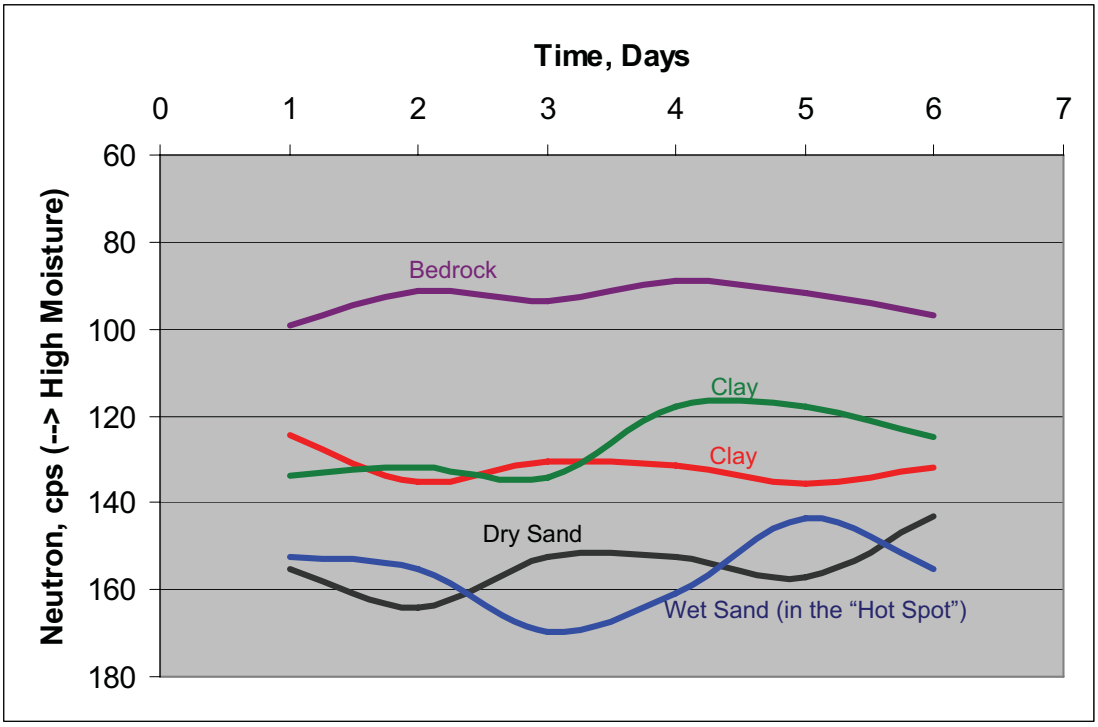

Figure 44. Graph. Moisture Monitoring of Abutment 1 Shaft 1. Hagerman National Wildlife Refuge, TX. Temperature Values are Averaged from the Four Access Tubes at 3m (Black), 6 m (Blue), 9 m (Red), 12 m (Green), and 15 m (Magenta) Depth Points.

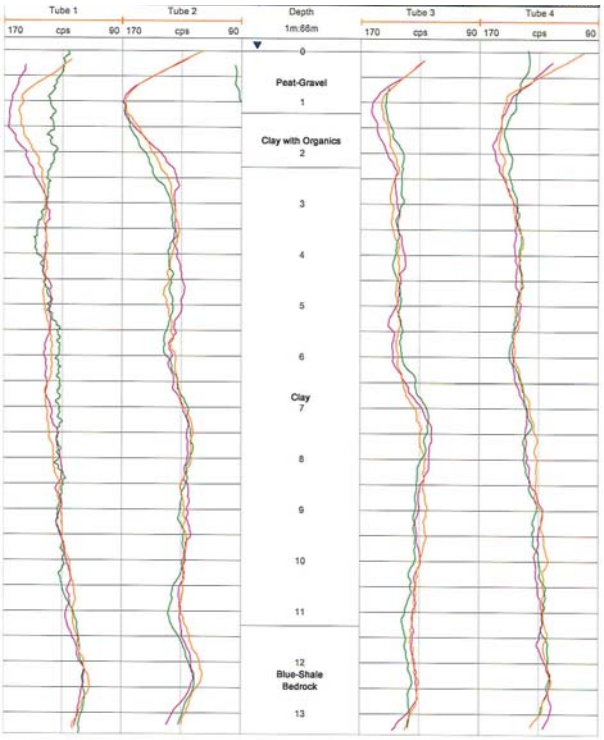

Figure 45. Plot. Moisture Monitoring of Pier 2 Shaft 2. Hagerman National Wildlife Refuge, TX. NML Moisture Curves at 2 Days (Green), 3 Days (Purple), and 4 Days (Orange) After the Concrete Placement. Vertical Guideline: 130 cps.